Chlamydia muridarum Evades Growth Restriction by the IFN-γ-Inducible Host Resistance Factor Irgb10[1]

Jörn Coers,* Isaac Bernstein-Hanley,* David Grotsky,* Iana Parvanova,† Jonathan C. Howard,‡ Gregory A. Taylor,§¶ William F. Dietrich,‖ and Michael N. Starnbach[2]*

Chlamydiae are obligate intracellular bacterial pathogens that exhibit a broad range of host tropism. Differences in host tropism between *Chlamydia* species have been linked to host variations in IFN-γ-mediated immune responses. In mouse cells, IFN-γ can effectively restrict growth of the human pathogen *Chlamydia trachomatis* but fails to control growth of the closely related mouse pathogen *Chlamydia muridarum*. The ability of mouse cells to resist *C. trachomatis* replication is largely dependent on the induction of a family of IFN-γ-inducible GTPases called immunity-related GTPases or IRGs. In this study we demonstrate that *C. muridarum* can specifically evade IRG-mediated host resistance. It has previously been suggested that *C. muridarum* inactivates the IRG protein Irga6 (Iigp1) to dampen the murine immune response. However, we show that Irga6 is dispensable for the control of *C. trachomatis* replication. Instead, an effective IFN-γ response to *C. trachomatis* requires the IRG proteins Irgm1 (Lrg47), Irgm3 (Igtp), and Irgb10. Ectopic expression of Irgb10 in the absence of IFN-γ is sufficient to reduce intracellular growth of *C. trachomatis* but fails to restrict growth of *C. muridarum*, indicating that *C. muridarum* can specifically evade Irgb10-driven host responses. Importantly, we find that Irgb10 protein intimately associates with inclusions harboring *C. trachomatis* but is absent from inclusions formed by *C. muridarum*. These data suggest that *C. muridarum* has evolved a mechanism to escape the murine IFN-γ response by restricting access of Irgb10 and possibly other IRG proteins to the inclusion. *The Journal of Immunology,* 2008, 180: 6237–6245.

Chlamydia trachomatis is an obligate intracellular bacterial pathogen that is the etiologic agent of prevalent human infections causing serious public health problems (1). Ocular infection with *C. trachomatis* is the leading cause of preventable blindness worldwide (2). Urogenital tract infection with *C. trachomatis* is the most common bacterial sexually transmitted disease in the United States and can lead to pelvic inflammatory disease, ectopic pregnancies, and infertility (3). The development of a vaccine against *C. trachomatis* infection has been complicated by the inability to genetically manipulate *C. trachomatis* and by the absence of a small animal model of *C. trachomatis* infection that adequately recapitulates human disease (4–6). A more thorough understanding the immune response to *C. trachomatis* in mice is a prerequisite for the development of a mouse model that better mimics human *C. trachomatis* infections.

All *Chlamydia* genera undergo a biphasic developmental cycle. Infection is initiated by the attachment of the highly infectious, metabolically inert elementary body to host cells. The elementary body subsequently facilitates its own uptake into a membrane-bound vesicle termed an inclusion (7). The inclusion evades fusion with the lysosome and the elementary body rapidly differentiates into a metabolically active reticulate body that replicates by binary fission within the protected environment of the inclusion (8). At the end of the developmental cycle the reticulate bodies differentiate back into elementary bodies, which subsequently egress from the host cell to initiate new rounds of infection.

The common cell biology of different *Chlamydia* sp. is likely to be based on the near synteny of the different *Chlamydia* genomes (9–11). For instance, the human pathogen *C. trachomatis* and the mouse pathogen *Chlamydia muridarum* share >99% of all predicted open reading frames and genetically diverge primarily in a small hypervariable region of the chromosome termed the plasticity zone (9). However, despite their extensive sequence homology and common cell biology, these two *Chlamydia* species display distinct host tropism (6).

Different aspects of host-pathogen interactions determine host tropism, including the adaption of pathogens to host-specific immune responses (5). A pivotal element of mammalian immunity consists of responses elicited by the cytokine IFN-γ. Accumulating evidence suggests that the ability of distinct *Chlamydia* sp. to circumvent host-specific IFN-γ responses plays an important role in determining host tropism (5, 12–15).

In human cells, an important mediator of cell-autonomous resistance to *C. trachomatis* is the induction of the enzyme IDO by IFN-γ. IDO catabolizes intracellular pools of tryptophan, thereby starving the pathogen of this essential amino acid (16, 17). Chlamydiae deprived of tryptophan enter a nonreplicating, persistent state (18, 19). However, genital *C. trachomatis* strains but not *C. muridarum* can overcome the IDO-dependent growth restriction. It

*Department of Microbiology and Molecular Genetics, Harvard Medical School, Boston, MA 02115; †Department of Molecular Pathology, University of Bern, Bern, Switzerland; ‡Institute for Genetics, University of Cologne, Cologne, Germany; §Departments of Medicine, Molecular Genetics and Microbiology, and Immunology, and Center for the Study of Aging, Duke University, Durham, NC 27708; ¶Geriatric Research and Education and Clinical Center, Veteran Affairs Medical Center, Durham, NC 27710; and ‖Mouse Genetics and Toxicology Models of Disease Center, Novartis Institutes for BioMedical Research, Cambridge, MA 02139

Received for publication November 21, 2007. Accepted for publication February 26, 2008.

The costs of publication of this article were defrayed in part by the payment of page charges. This article must therefore be hereby marked *advertisement* in accordance with 18 U.S.C. Section 1734 solely to indicate this fact.

[1] This work was supported by National Institutes of Health Grants AI062827 (to M.N.S.), AI57831 (to G.A.T.), a Veteran Affairs Merit Review Grant (to G.A.T.), and the SFB670 Grant "Cell Autonomous Immunity" (to J.C.H.). J.C. was supported by a research fellowship from the Deutsche Forschungsgemeinschaft and by the Charles A. King Trust Postdoctoral Research Fellowship.

[2] Address correspondence and reprint requests to Dr. Michael N. Starnbach, Harvard Medical School, 200 Longwood Avenue, Boston, MA 02115. E-mail address: starnbach@hms.harvard.edu

has been found that *C. trachomatis* strains isolated from the human urogenital tract express tryptophan synthase, an enzyme capable of using exogenous indole for the synthesis of tryptophan (14, 20). Supplementing indole can restore the capacity of *C. trachomatis* genital isolates to replicate in IFN-γ-treated human cells (20). The ability to synthesize tryptophan may allow *C. trachomatis* strains to escape IFN-γ-mediated suppression in the genital tract by using indole provided by the local microbial flora. In contrast, *C. muridarum* lacks a functional tryptophan synthase and supplementing indole does not restore bacterial growth in IFN-γ-treated human cells (9, 14).

In mouse cells, growth of *C. trachomatis* and *C. muridarum* is also differentially affected by IFN-γ treatment. In most murine cell lines, IFN-γ treatment drastically reduces growth of *C. trachomatis* but not *C. muridarum* (13, 14). A family of IFN-γ-inducible p47 GTPases termed immunity-related GTPases (IRGs)[3] has been implicated in IFN-γ-mediated suppression of *C. trachomatis* growth in mouse cells (13, 21). We have previously shown that mouse embryonic fibroblasts (MEFs) depleted of Irgb10 mRNA by RNA interference (RNAi) or carrying a targeted gene deletion of *Irgm3* are defective in IFN-γ-mediated resistance to *C. trachomatis* (21). In a separate study, Nelson et al. showed that transfection with RNAi oligonucleotides targeting Irga6 led to a 2- to 3-fold increase in recoverable inclusion-forming units in IFN-γ activated mouse epithelial cells (13). The authors suggested that the gene *TC438* encoded in the plasticity zone of *C. muridarum* but absent from the *C. trachomatis* genome is responsible for immune evasion by *C. muridarum* in mice. *TC438* encodes a large protein with homology to the UDP-glycosyltransferase portion of the large clostridial toxin and the *Yersinia* virulence factor YopT. The *Yersinia* effector YopT acts as a cysteine protease to remove the lipid modification from Rho GTPases at a cleavage site that is just N-terminal from the cysteine linked to the prenyl group (22). This cleavage releases the GTPase from the membrane and inactivates it. Nelson et al. suggested that TC438 inactivates the GTPase Irga6 by a similar proteolytic mechanism (13).

To test the hypothesis that *C. muridarum* interferes with Irga6 function, we first set out to confirm the role for Irga6 as a host factor that conveys resistance to *C. trachomatis* growth. Surprisingly, we found that mice carrying a gene deletion of *Irga6* were as resistant to *C. trachomatis* infections as coisogenic C57BL/6 (B6) mice both in a systemic infection model in vivo and in IFN-γ-treated cells ex vivo. Instead, we found that the IRG family members Irgb10, Irgm1, and Irgm3 are required for resistance to *C. trachomatis*. We demonstrate that ectopic expression of Irgb10 in the absence of a general IFN-γ response is sufficient to reduce bacterial yield of *C. trachomatis* but not *C. muridarum*. The differential effect of Irgb10 expression on *Chlamydia* growth correlated with the distinct subcellular localization of Irgb10 in cells infected with *C. trachomatis* as compared with those infected with *C. muridarum*. Specifically, we show that Irgb10 protein decorates an inclusion formed by *C. trachomatis*, whereas Irgb10 is absent from *C. muridarum* inclusions. Therefore, we suggest a model in which Irgb10 is required to localize to the inclusion to limit bacterial replication and propose that *C. muridarum* has evolved a mechanism to restrict access of IRG proteins to its inclusion.

[3] Abbreviations used in this paper: IRG, immunity-related GTPase; B6, C57BL/6; hpi, hours postinfection; MEF, mouse embryonic fibroblast; MOI, multiplicity of infection; MOMP, major outer membrane protein; RNAi, RNA interference.

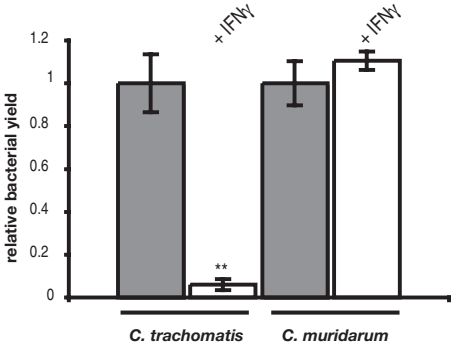

FIGURE 1. *C. muridarum* evades the IFN-γ response in MEFs. MEFs were treated for 15 h with either 100 or 10^3 U/ml IFN-γ and then infected with either *C. trachomatis* or *C. muridarum* at an MOI of 1. At 29 hpi cells were harvested and bacterial yield was determined using quantitative PCR. The amount of bacterial yield in IFN-γ-treated cells is shown relative to that in the untreated control. Each bar represents the mean bacterial yield of three independently infected wells. Bacterial yield of *C. trachomatis* in IFN-γ-treated cells was significantly reduced compared with bacterial yield in untreated cells ($p \leq 0.005$).

Materials and Methods

Mice

All mice were maintained and bred under specific pathogen-free conditions. All experiments were approved by the Institutional Animal Care and Use Committee of Harvard Medical School (Boston, MA). Control B6 and B6.129S2-*Irf1* mice were obtained from The Jackson Laboratory. The targeted gene deletions of *Irgm1* and *Irgm3* have been described previously (23, 24). *Irgm1*$^{-/-}$ and *Irgm3*$^{-/-}$ mice used in this study were backcrossed for >10 generations to B6. The *Irgm1*$^{-/-}$ mice used in this study carry the B6 alleles of the IRG genes, *Irgm2, Irgm3*, and *Irgb10*. The *Irgm3*$^{-/-}$ mice carry the 129 alleles of *Irgm2* and *Irgb10* (data not shown). *Irga6*$^{-/-}$ mice have also been described previously (25) and were generated in B6-derived (Bruce4) embryonic stem cells. The third exon encoding the whole open reading frame of Irga6 was flanked by LoxP sites and deleted in vivo by crossing to Cre-deleter mice (26). A congenic mouse strain that carries a small 129 genomic interval encompassing the *Ctrq3* locus (B6.*Ctrq3*^{129}) was generated by taking advantage of the fact that most mouse knockout strains have been made using 129-derived embryonic stem cell lines and subsequently backcrossed to B6 mice, thus creating 129 congenic mice on a B6 background. To make the B6.*Ctrq3*^{129} strain, the congenic mouse strain B6.129S2-*Irf1* carrying a targeted gene deletion in *Irf1* on chromosome 11 was further backcrossed to B6 to generate mice that had lost the *Irf1* knockout allele but still carried an interval of 129-derived DNA on chromosome 11 surrounding the *Ctrq3* locus. These mice were then intercrossed to generate mice homozygous for the *Ctrq3*^{129} allele. The 129 genomic interval of the B6.*Ctrq3*^{129} mice encompasses 2.1 Mb of DNA containing the 129 alleles of *Irgm2* and *Irgb10* and is flanked by the markers D11Zbh3 and D11Zbh5 (data not shown).

Genetic markers and genotyping

Genotyping of the knockout alleles for *Irgm1* and *Irgm3* was performed as described previously (23, 24). Simple sequence length polymorphism markers were used to determine the boundaries of congenic intervals as described previously (21). Primer sequences for marker D11Zbh3 has previously been reported (21). The primer sequences for marker D11Zbh5 are as follows: D11Zbh5 forward, 5′-AATGGAGGTCCAGTGTTACTGC-3′; D11Zbh5 reverse, 5′-TTGAACAGAATCAACAGCAACC-3′.

Chlamydia *strains and evaluation of bacterial yield*

C. trachomatis serovar L2 434/Bu and *C. muridarum* were propagated in McCoy cells and purified as described (27, 28). To quantify the bacterial load in *Chlamydia*-infected cells and in the spleens of infected animals, a previously described quantitative PCR assay was applied (27). Briefly, total nucleic acid from infected cells or spleen homogenates was prepared using the QIAamp DNA mini kit from Qiagen. *Chlamydia* 16S DNA and mouse GAPDH DNA content of individual samples was then quantified by quantitative PCR on an ABI 7000 sequence detection system using primer pairs and dual-labeled probes. Standard curves were generated from known

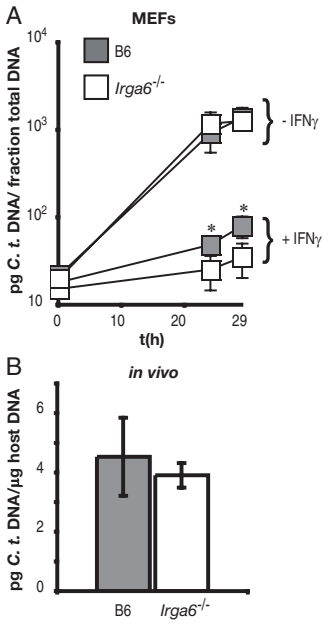

FIGURE 2. *Irga6* knockout mice are highly resistant to *C. trachomatis* (*C. t.*) infections. *A*, IFN-γ activated and untreated MEFs of the indicated genotype were infected with *C. trachomatis* at an MOI of 1 and cells were harvested at 29 hpi. Each data point represents the mean bacterial yield of three independently infected wells. Irga6 knockout cells were significantly more resistant to *C. trachomatis* growth than B6 cells ($p \leq 0.05$). *B*, For systemic in vivo infections, four mice of the indicated genotypes were i.v. injected with *C. trachomatis*. The mean bacterial yield in spleens at 29 hpi is shown (pg, picograms; µg, micrograms).

amounts of *Chlamydia* and mouse DNA, and these curves were used to calculate the amount (in picograms) of *Chlamydia* DNA per unit weight (in micrograms) of mouse DNA in the samples. For in vitro experiments, bacterial yield is shown relative to a control sample in arbitrary units with the control being equal to 1.

Chlamydia *infections*

Unless stated otherwise, cells were treated with 100 U/ml rIFN-γ (Invitrogen) for 15 h before infection or left untreated. Cells were infected with *Chlamydia* at a multiplicity of infection (MOI) of 1 in SPG buffer (220 mM sucrose, 12.5 mM phosphate, and 4 mM L-glutamic acid (pH 7.5)) by centrifugation at 1928 × *g* for 1 h at 37°C and then returned to standard medium. At 29 h postinfection (hpi) cells were harvested and bacterial yield was determined as described above. All experiments were conducted in triplicate. Mice, 6- to 8-wk old, had 10^7 inclusion-forming units of *C. trachomatis* L2 in 200 µl of SPG buffer injected into the tail vein. At least three mice per genotype were used for each experiment. At 29 hpi mice were sacrificed and the splenic bacterial load was determined as previously described (27).

Cell culture, Abs, Irgb10-GFP, and microscopy

MEFs were generated from the indicated mouse strains as previously described (27). Cell lines were cultured according to the standard protocols provided by the American Tissue Culture Collection. Retroviral transduction of MEFs was conducted using a mouse stem cell virus vector. For immunofluorescence studies, cells were grown and infected on glass coverslips. Cells were fixed in methanol for 5 min, washed in PBS, and blocked with 5% goat serum. For *C. trachomatis* infections, cells were stained with a mouse mAb against the *C. trachomatis* major outer membrane protein (MOMP; Accurate Chemical and Scientific). For *C. muridarum* infections, cells were stained with a mouse mAb to *Chlamydia* LPS (RDI-Fitzgerald) or a mouse monoclonal anti-MOMP Ab specific for *C. muridarum* (29). An affinity-purified polyclonal rabbit anti-Irgb10 Ab was generated against the C-terminal peptide LKKKVFLQDSVDSE of Irgb10 and used to detect Irgb10 by microscopy. The following Abs were used to stain for additional IRG proteins: rabbit anti-Irga6 165 (30), goat anti-Irgm1 A19 (Santa Cruz Biotechnology), mouse anti-Irgm1 (31), mouse anti-Irgm3 I68120 (BD-Transduction Labs), and rabbit anti-Irgm3 (32). Primary Abs were visualized by staining with secondary FITC- or rhodamine red X-conjugated donkey anti-rabbit IgG or anti-mouse IgG (Jackson ImmunoResearch Laboratories). To determine the localization of Irgb10 in *C. trachomatis*/*C. muridarum* coinfections, fixed cells were labeled with rabbit anti-Irgb10 Ab and mouse anti-MOMP Ab specific for *C. muridarum* (29). Primary Abs were visualized by staining with secondary rhodamine red X-conjugated donkey anti-rabbit IgG and either Cy5- or 7-amino-4-methylcoumarin-3-acetic acid (ACMA)-conjugated donkey anti-mouse IgG. Subsequently, cells were stained with FITC-coupled mouse anti-MOMP Ab specific for *C. trachomatis*. To visualize Irgb10 protein directly, the B6 cDNA of Irgb10 was cloned into the vector pEGFP-N2 (Invitrogen). The generated vector encodes Irgb10 with a C-terminal GFP moiety and was transfected into cells using FuGene6 (Invitrogen) according to the manufacturer's protocol. All epifluorescent images were acquired with a Nikon Eclipse TE2000-U microscope and Plan Fluor ELWD ×60 objective. Images were saved as TIFF files and imported into Adobe Illustrator for labeling.

Statistical analysis

All comparisons were evaluated for statistical significance through the use of unpaired two-tailed *t* tests. Where it appeared necessary to highlight significant differences between data points, the level of significance is depicted by ∗ for $p \leq 0.05$ and ∗∗ for $p \leq 0.005$.

Results

IFN-γ activated MEFs fail to restrict growth of C. muridarum

IFN-γ treatment of most murine cells activates a highly effective antibacterial response to *C. trachomatis* but fails to restrict growth of *C. muridarum.* We and others have investigated whether IRG proteins are required to restrict the growth of *C. trachomatis* in mouse cells (13, 21). It has been suggested that *C. muridarum* targets and inactivates IRG proteins to overcome the murine IFN-γ response (13); however, no experimental evidence has been provided to support this hypothesis. To investigate the mechanism by which *C. muridarum* evades cell-autonomous immune restriction, we first tested whether *C. muridarum* can escape the IFN-γ response in MEFs, a cell type that requires the IRG proteins Irgb10

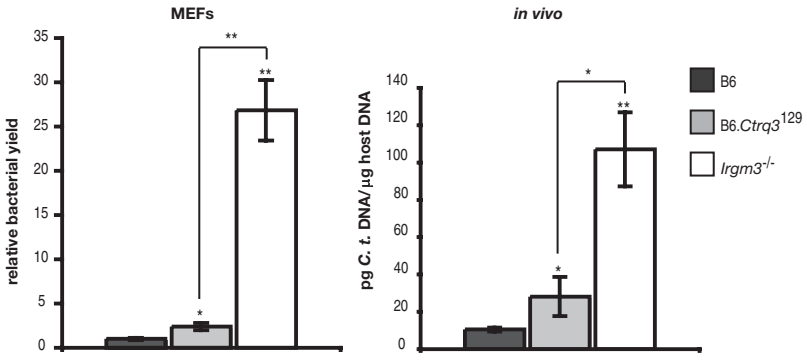

FIGURE 3. The increased susceptibility of *Irgm3* knockout mice is predominantly due to the deletion of *Irgm3*. IFN-γ activated MEFs of the indicated genotype were infected with *C. trachomatis* (*C. t.*) at an MOI of 1 and cells were harvested at 29 hpi. The bacterial yield of three independently infected wells is shown relative to B6 control cells (pg, picograms; µg, micrograms). The same mouse strains were tested for their susceptibility to *C. trachomatis* infections in vivo. Statistically significant differences to B6 mice and between the *Irgm3* knockout and the B6.*Ctrq3*^{129} congenic mice are highlighted through the use of asterisks (∗, $p \leq 0.05$; ∗∗, $p \leq 0.005$).

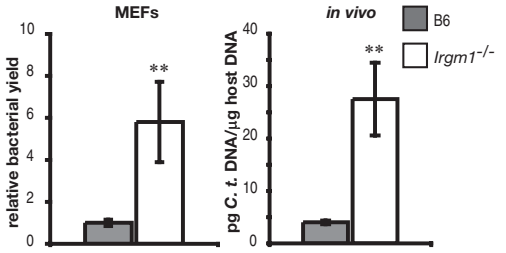

FIGURE 4. *Irgm1* knockout mice display increased susceptibility to *C. trachomatis* (*C. t.*) infections. IFN-γ-activated MEFs of the indicated genotype were infected with *C. trachomatis* at an MOI of 1 and the cells were harvested at 29 hpi. The amount of bacterial yield in *Irgm1* knockout cells is shown relative to that of B6 control cells (pg, picograms; µg, micrograms). The experiment was performed in triplicate. *Irgm1* knockout mice and B6 controls were also tested for their susceptibility to *C. trachomatis* infections in vivo. Statistically significant differences to B6 mice and cells are highlighted (**, $p \leq 0.005$).

and Irgm3 for resistance to *C. trachomatis* (21). As we have shown previously, B6 MEFs treated with 100 U/ml IFN-γ became highly resistant to *C. trachomatis* growth (21, 27). Bacterial yield from IFN-γ-treated B6 MEFs was ~20-fold lower than the yield from untreated cells at 29 hpi (Fig. 1). In contrast, *C. muridarum* growth was impervious to IFN-γ treatment, even at high cytokine concentrations of 10^3 U/ml (Fig. 1). MEFs therefore can be used as a model system to study immune evasion by *C. muridarum.*

Irga6 is not required for the immune response to C. trachomatis

Studies by Nelson et al. showed that an RNAi oligonucleotide duplex targeting Irga6 partially reverted IFN-γ-induced growth inhibition of *C. trachomatis* in mouse oviduct epithelial cells (13). The authors therefore suggested that *C. muridarum* blocks the function of Irga6 protein to overcome the cell-autonomous immune restriction imposed by IFN-γ activation (13). In this study, we used a recently described mouse strain carrying a *Irga6* knockout allele in a pure B6 genetic background (25). Surprisingly, we found that *Irga6*$^{-/-}$ MEFs were not defective but more efficient in restricting growth of *C. trachomatis* compared with B6 control MEFs in IFN-γ-treated but not untreated cells (Fig. 2*A*). Moreover, in systemically infected mice the splenic *C. trachomatis* loads of *Irga6*$^{-/-}$ mice were not significantly different from the bacterial yields in B6 mice (Fig. 2*B*) These data collectively show that *Irga6* is not required for the immune response to *C. trachomatis* and that the Irga6 protein is unlikely to be the main target of the immune evasion mechanism used by *C. muridarum.*

Irgm3 and Irgm1 are required for complete immune restriction of C. trachomatis *growth*

Previously, we mapped a small 1.3-Mb genetic interval derived from mouse strain C3H/HeJ that conveys susceptibility to *C. trachomatis* replication both in MEFs and in a systemic infection model (21, 27). This locus, termed *Ctrq3*, contains the IRG genes *Irgb10, Irgm2,* and *Irgm3* (21, 33). We have previously shown that IFN-γ-treated *Irgm3*$^{-/-}$ MEFs are more susceptible to *C. trachomatis* replication than B6 MEFs (21). Similarly, a recent study found that *Irgm3*$^{-/-}$ mice are more susceptible to *Chlamydia psittaci* infections (33). Because the *Irgm3* knockout allele was generated in 129-derived embryonic stem cell (24), *Irgm3*$^{-/-}$ mice on a B6 genetic background carry an *Irgm3* knockout allele that is flanked by 129-derived DNA encompassing the 129 alleles of *Irgm2* and *Irgb10* (data not shown). Miyairi et al. raised the interesting possibility that the phenotype of the *Irgm3*$^{-/-}$ mice was due to the 129 alleles of *Irgm2* and/or *Irgb10* rather than the

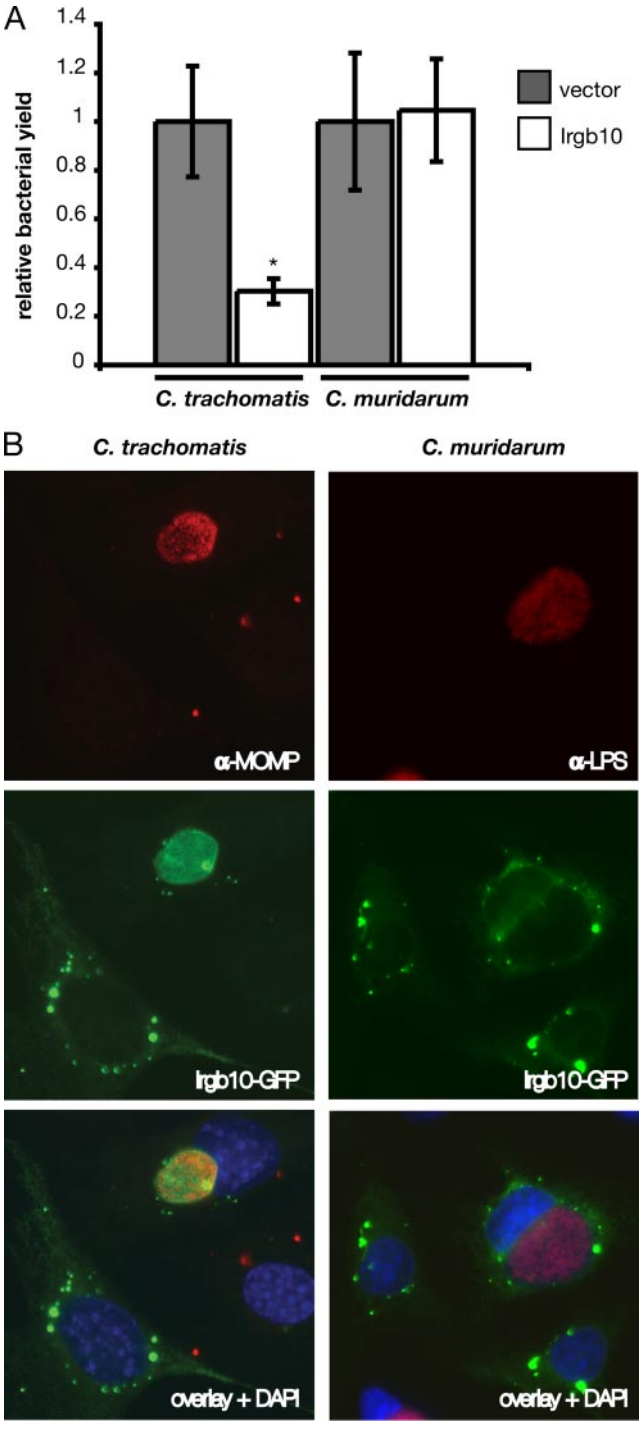

FIGURE 5. Ectopically expressed Irgb10 negatively affects bacterial yield of *C. trachomatis* but not *C. muridarum* and specifically localizes to *C. trachomatis* inclusions. *A*, MEFs were retrovirally transduced with mouse stem cell virus-expressing IRES-GFP (vector) or Irgb10-IRES-GFP (Irgb10) (where IRES is internal ribosome entry site). Transduction efficiency was >90% as determined by flow cytometry (data not shown). Cells were then infected with either *C. trachomatis* or *C. muridarum* at an MOI of 1 and cells were harvested at 29 hpi. The amount of bacterial yield is shown relative to IRES-GFP-transduced control cells. The experiment shown was performed in triplicate (*, $p \leq 0.05$). *B*, MEFs were transiently transfected with Irgb10-GFP and then infected with either *C. trachomatis* or *C. muridarum* at an MOI of 1. Cells were prepared for fluorescent microscopy at 24 hpi. Representative images of infected and uninfected Irgb10-GFP$^+$ cells are shown. DAPI, 4′,6-diamidino-3-phenylindole; α, anti.

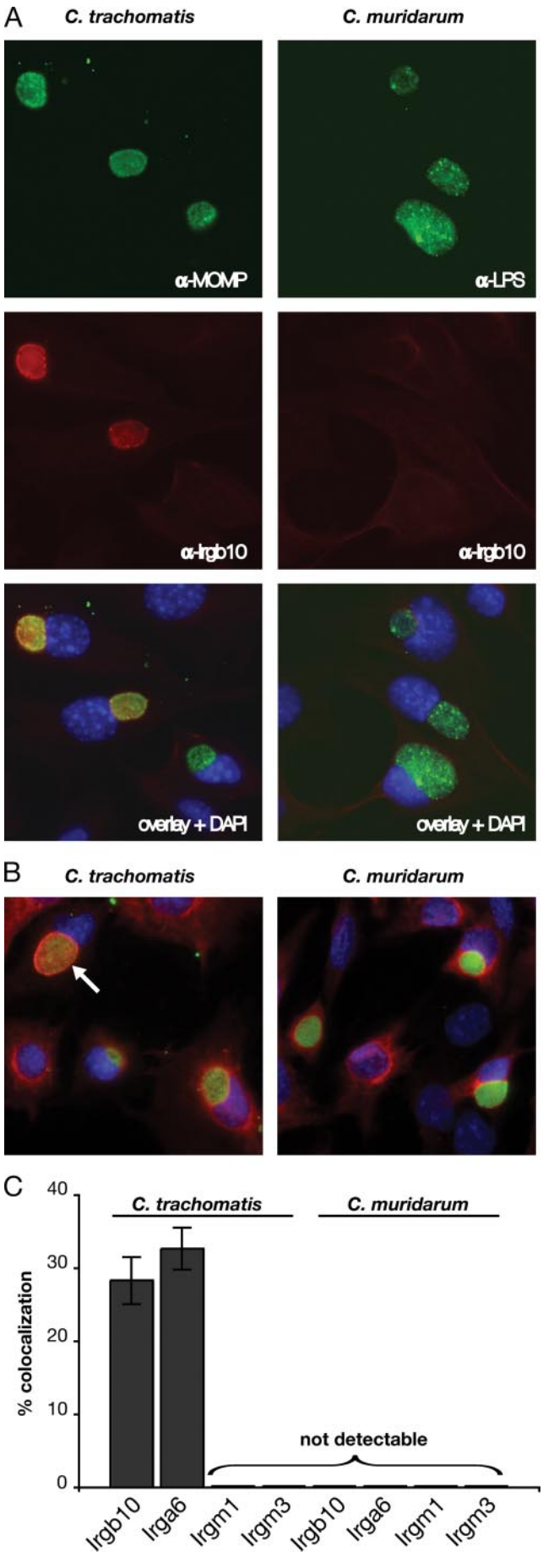

targeted gene deletion of *Irgm3* itself (33). To test this hypothesis, we generated a congenic mouse strain that carries a 2.1-Mb 129-derived DNA interval encompassing the genes *Irgb10*, *Irgm2*, and *Irgm3* on a B6 genetic background (B6.*Ctrq3*^{129}). IFN-γ-treated MEFs derived from the congenic B6.*Ctrq3*^{129} mice allow ~3-fold more *C. trachomatis* replication than B6 MEFs (Fig. 3). This result strongly suggests that both the C3H and the 129 alleles of *Ctrq3* confer increased susceptibility to *C. trachomatis* infections compared with the B6 *Ctrq3* allele, although we currently do not know whether the same polymorphisms are responsible for the increased susceptibility conveyed by the 129 and C3H alleles of *Ctrq3*. Importantly, IFN-γ-treated *Irgm3*$^{-/-}$ MEFs were nearly 10-fold more susceptible to *C. trachomatis* growth than B6.*Ctrq3*^{129} MEFs, indicating that the *Irgm3* knockout allele itself also conveys increased susceptibility to *C. trachomatis* infections. We next tested the role of *Irgm3* in controlling systemic *C. trachomatis* infections. Similar to the results obtained in MEFs, *Irgm3*$^{-/-}$ mice were significantly more susceptible than B6.*Ctrq3*^{129} mice, and both *Irgm3*$^{-/-}$ and B6.*Ctrq3*^{129} mice displayed deficiencies in their early immune responses to *C. trachomatis* compared with B6 mice (Fig. 3). Collectively, these results indicate a pivotal role of *Irgm3* in the innate immunity of mice to *C. trachomatis*.

Based on the GTPase motif sequence, *Irgm1* and *Irgm2* are the closest homologues of *Irgm3* and, therefore, are also attractive candidates as mediators of host resistance to *C. trachomatis* (34). An *Irgm2*$^{-/-}$ mouse has not been reported to exist, but *Irgm1*$^{-/-}$ mice have been shown to display decreased resistance against all intracellular bacterial pathogens tested to date (23, 35–40). The *Irgm1*$^{-/-}$ mice used in our experiments have been backcrossed for 12 generations and carry the B6 allele of *Ctrq3* (data not shown). Both in IFN-γ activated MEFs and in systemically infected mice *Irgm1*$^{-/-}$ mice displayed a 5- to 6-fold increase in *C. trachomatis* yield at 29 hpi (Fig. 4). These data establish that, similar to *Irgm3, Irgm1* is also important in resistance to infections with *C. trachomatis*.

Ectopic expression of Irgb10 restricts growth of C. trachomatis *but not* C. muridarum

Twenty-three IRG genes exist in the mouse genome and the majority of these genes have been shown to be IFN-γ inducible (34). The data shown above and in our previous work demonstrate that at least three IRG proteins are required for an efficient early immune response to *C. trachomatis* (21, 27). However, in the human genome only two IRG genes exist, neither of which are induced upon IFN-γ stimulation (34). Because IFN-γ-mediated induction of IRG genes is only seen in mouse and not in human cells, we hypothesized that one or more IRG genes are the primary targets of the immune evasion mechanism used by *C. muridarum.* To test

FIGURE 6. Endogenous Irgb10 and Irga6 decorate inclusions formed by *C. trachomatis* but not *C. muridarum.* MEFs were infected with either *C. trachomatis* or *C. muridarum* at an MOI of 1 and treated with 100 U/ml IFNγ at the time of infection. *A*, At 24 hpi cells were prepared for microscopy and representative images are shown. In the *left column*, two of three *C. trachomatis* inclusions strongly associate with Irgb10. In the *right column*, none of the *C. muridarum* inclusions stain positive for Irgb10. *B*, Cells harvested at 20 hpi were stained for *Chlamydia* (green), Irga6 (red), and DNA (blue). Representative images are shown and the white arrow in the *left panel* marks an inclusion colocalizing with Irga6. *C*, For each of the indicated IRG proteins three independently infected wells were analyzed for colocalization with either *C. trachomatis* or *C. muridarum* inclusions at 20 hpi. In each well, 100 randomly selected inclusions were visually scored for colocalization with IRG proteins. The results are representative of at least two independent experiments conducted for each IRG protein.

this hypothesis, we first attempted to restrict *Chlamydia* growth by ectopic expression of individual IRG proteins in the absence of IFN-γ stimulation. We found that ectopic expression of either Irgm1 or Irgm3 alone had no discernible effect on *C. trachomatis* growth (data not shown). However, expression of Irgb10 in MEFs (Fig. 5*A*) or 3T3 cells (data not shown) resulted in a relatively small but reproducible 2- to 3-fold reduction in *C. trachomatis* yield at 29 hpi. Importantly, expression of Irgb10 had no effect on *C. muridarum* growth (Fig. 5*A*). These data show that in the absence of other effects that might be induced by IFN-γ, Irgb10 expression alone is sufficient to moderately reduce the growth of *C. trachomatis* but not *C. muridarum*.

Irgb10 and Irga6 associate with inclusions formed by C. trachomatis *but not by* C. muridarum

Most IRG proteins examined to date have been found to localize to diverse membrane compartments and to associate with the pathogen-containing vacuole of organisms like *Toxoplasma gondii* and *Mycobacterium tuberculosis* (25, 30, 31, 37, 41–44). Results from these studies imply that localization to the pathogen-containing vacuole is essential for the antimicrobial effector function of at least a subset of IRG proteins. We therefore examined the subcellular localization of Irgb10 in *C. trachomatis*-infected cells using an Irgb10 protein fused to GFP at its C terminus. In *C. trachomatis*-infected cells, we found Irgb10-GFP intimately associated with the inclusion (Fig. 5*B*). In contrast, Irgb10-GFP was absent from *C. muridarum*-containing inclusions (Fig. 5*B*). Noticeably, ectopic expression of Irgb10-GFP led to the formation of large Irgb10-GFP aggregates in uninfected cells (Fig. 5*B*). Similar to the effect of IFN-γ on aggregates formed by ectopically expressed Irga6 (38), stimulation of MEFs with IFN-γ led to the disappearance of Irgb10-GFP aggregates and dispersion of Irgb10-GFP throughout the cell (data not shown). These data indicate that the subcellular localization of Irgb10 is regulated by additional IFN-γ-inducible factors. To determine the subcellular localization of Irgb10 during the IFN-γ response, we labeled for endogenous Irgb10 using a polyclonal Ab directed against the very C-terminal peptide of Irgb10. IFN-γ-activated, uninfected cells displayed weak staining with anti-Irgb10 that could not be clearly associated with any particular intracellular structure (Fig. 6*A* and data not shown). However, in *C. trachomatis*-infected cells the localization of Irgb10 to the inclusion could be observed as early as 10 hpi and throughout the course of the infection (Fig. 6*A* and data not shown). At 20 and 24 hpi, 30 - 40% of the *C. trachomatis* inclusions stained positive for Irgb10 (Fig. 6*C* and Fig. 7). In contrast, after examining >1,000 inclusions we never found Irgb10 to be associated with *C. muridarum* (Fig. 6 and data not shown).

To determine whether *C. muridarum* restricts the access of additional IRG proteins to its inclusions, we analyzed the subcellular localization of the IRG proteins Irgm1, Irgm3, and Irga6 in *C. trachomatis*- and *C. muridarum*-infected cells. For Irgm1 and Irgm3 we were not able to detect colocalization with inclusions formed by either *Chlamydia* species at multiple time points postinfection (7, 16, 20, and 24 hpi) using two distinct Abs for each protein (Fig. 6*C* and data not shown). The IRG protein Irga6, in contrast, associated with *C. trachomatis* at a frequency similar to that of Irgb10 but was absent from *C. muridarum* inclusions (Fig. 6, *B* and *C*). These results demonstrate that Irgb10 and Irga6, two IRG proteins strongly associated with *C. trachomatis* inclusions, fail to accumulate at inclusions formed by *C. muridarum.*

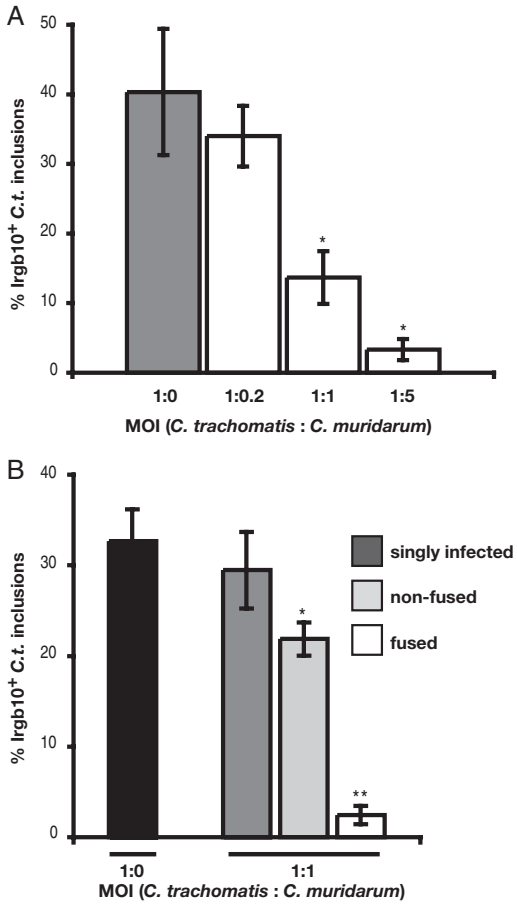

FIGURE 7. *C. muridarum* restricts the acquisition of Irgb10 to *C. trachomatis* (*C. t.*)-containing inclusions in coinfected cells. MEFs were coinfected with *C. trachomatis* and *C. muridarum* at the indicated MOI and treated with IFN-γ at the time of infection. Cells were stained to identify *C. trachomatis*-containing inclusions and determine Irgb10 localization as described in *Materials and Methods*. *A*, Three independently infected wells were analyzed per data point. In each well, 100 randomly selected *C. trachomatis* inclusions were visually scored for colocalization with Irgb10. *B*, Cells were stained using species-specific anti-MOMP Abs to distinguish cells that were infected with *C. trachomatis* alone (singly infected) from cells that were infected with both *C. trachomatis* and *C. muridarum.* Within cells infected with both *Chlamydia* species, *C. trachomatis*-containing inclusions were visually inspected to determine the absence (nonfused) or presence (fused) of *C.* muridarum within the same inclusion. Three independently infected wells were analyzed per data point. In each well at least 20 inclusions of each category (singly infected, nonfused, and fused) were visually scored for the presence of Irgb10. Statistically significant differences to cells infected with *C. trachomatis* alone are highlighted (*, $p \leq 0.05$; **, $p \leq 0.005$).

Coinfection with C. muridarum *reduces the number of Irgb10-positive* C. trachomatis *inclusions*

It has recently been reported that coinfection with *C. muridarum* protects *C. trachomatis* inclusions from IFN-γ-mediated growth restriction in mouse cells (45). To examine whether the inhibition of Irgb10 function may be involved in the rescue of *C. trachomatis* growth by *C. muridarum*, we tested whether coinfection with *C. muridarum* also restricts the access of Irgb10 to *C. trachomatis* inclusions. To specifically identify inclusions harboring *C. trachomatis*, we stained cells with a species-specific anti-MOMP Ab that detects *C. trachomatis* but not *C. muridarum*. We observed that coinfection with *C. muridarum* significantly decreased the number of Irgb10-positive *C. trachomatis* inclusions in a dose-dependent

manner (Fig. 7*A*). To determine whether *C. muridarum* must reside in the same cell as *C. trachomatis* to restrict the access of Irgb10 to the *C. trachomatis* inclusion, we triple-stained coinfected cells with anti-Irgb10 and two anti-MOMP Abs that distinguish between the two *Chlamydia* species. Our data show that colocalization of Irgb10 with *C. trachomatis* inclusions is exclusively reduced in cells harboring both *Chlamydia* strains. The most dramatic reduction in Irgb10 colocalization is seen with *C. trachomatis* inclusions that have fused with *C. muridarum* inclusions (Fig. 7*B*). Collectively, these data suggest that *C. muridarum* can actively block the acquisition of Irgb10 protein to *Chlamydia* inclusions and thus avoid an Irgb10-mediated antibacterial response.

Discussion

Bacterial pathogens have evolved a large repertoire of mechanisms to subvert both innate and adaptive immune reactions (46, 47), including the evasion of the NO synthase-dependent effector branch of the IFN-γ response (48). In this report we demonstrate that bacterial pathogens can directly counteract the IRG-dependent arm of the IFN-γ response. Specifically, we show that the mouse pathogen *C. muridarum* can evade an antimicrobial response driven by the IRG protein Irgb10.

It has previously been reported that *C. muridarum* but not *C. trachomatis* is resistant to the cell-autonomous antibacterial effect of IFN-γ in mouse cells, and it has been suggested that the specific inhibition of the IRG protein Irga6 by *C. muridarum* is the underlying cause for the resistance (13). However, no conclusive experimental evidence to support this model has been provided. In our study we used *Irga6* knockout mice to show that Irga6 is not required for the IFN-γ response to *C. trachomatis* in fibroblasts and splenocytes and thus conclude that *C. muridarum* is unlikely to evade the IFN-γ response in mouse cells through the inhibition of Irga6. The discrepancy of our results with the previous report by Nelson et al. (13) may indicate a unique requirement for Irga6 in resistance to *C. trachomatis* in epithelial cells. Alternatively, technical differences between the two studies could explain the divergent findings; whereas we analyzed knockout mice, Nelson et al. based their conclusions on the effect of a single RNAi oligonucleotide pair targeting Irga6 (13), an experimental approach that frequently produces off-target effects (49, 50).

Surprisingly, we found that the absence of Irga6 enhances the IFN-γ response to *C. trachomatis* in MEFs. At least two distinct but not mutually exclusive scenarios may explain the observed phenotype. Irga6 has previously been shown to multimerize (51), and it has been suggested that IRG proteins may engage in direct heteromeric interactions with one another (38). Accordingly, Irgb10 and Irga6 could be competing for binding partners (in particular, other IRG proteins) and Irgb10 may acquire these common binding partners more effectively in *Irga6*$^{-/-}$ MEFs. Additionally, our data show that Irga6 can access the inclusion, even though Irga6 is not required for the restriction of *C. trachomatis* growth by IFN-γ. Consequently, the absence of Irga6 may allow Irgb10 to access the inclusion more effectively. Although our data suggest that *Irga6*$^{-/-}$ and B6 mice are similarly susceptible to systemic infections with *C. trachomatis*, a more careful analysis of the in vivo phenotype (including the analysis of additional time points and bacterial load in other organs) is required to ultimately resolve this issue.

We have previously shown that another IRG protein, Irgb10, plays a central role in IFN-γ-dependent resistance to *C. trachomatis* in mice (21, 27). In this report we make the striking observation that Irgb10 colocalizes with *C. trachomatis* inclusions but is not detectable at *C. muridarum* inclusions. Similarly, Irga6 associates with *C. trachomatis* but not *C. muridarum* inclusions. We therefore suggest that *C. muridarum* escapes the IRG-mediated antibacterial immune response by disallowing Irgb10 and possibly other IRGs access to its inclusion.

In contrast to Irgb10 and Irga6, we did not observe any association of Irgm1 and Irgm3 with *Chlamydia* inclusions. Analogous to our findings, it has previously been reported that Irgm1 does not localize to the parasitophorous vacuole harboring *T. gondii,* although Irgm1 is required for growth restriction of this parasite (31). Collectively, these observations suggest that the localization of Irgm proteins to pathogen-containing vacuoles is not essential for this subclass of IRG proteins to act as resistance factors.

Two mechanistically distinct models could explain the differential localization of Irgb10 in *C. trachomatis*- and *C. muridarum*-infected cells. In the first model, Irgb10 protein recognizes properties specific to *C. trachomatis* inclusions. In support of this model, inclusions from *C. trachomatis* and *C. muridarum* have been reported to show some differences in their protein composition. For instance, the small Ras-like GTPase Rab6 is associated with *C. trachomatis* but not *C. muridarum* inclusions (52). However, we do not favor this model because identical IRG proteins appear to localize to vastly different vacuoles surrounding different intracellular pathogens (25, 37, 38, 41). This also appears to hold true for Irgb10, which not only localizes to the *C. trachomatis* inclusion but to at least one more vacuole engulfing a pathogen, namely the parasitophorous vacuole of *T. gondii* (J. C. Howard, unpublished data). Moreover, inclusions containing *C. trachomatis* can evade targeting by Irgb10 in cells coinfected with *C. muridarum.* These data strongly suggest that *C. muridarum* actively inhibits the localization of Irgb10 to the *Chlamydia* inclusion.

We therefore favor a second model in which *C. muridarum* actively constrains access of Irgb10 to its inclusion, either by removing Irgb10 from the inclusion membrane or by preemptively blocking trafficking of Irgb10 to the inclusion. Mechanistically, inhibition of Irgb10 membrane targeting could be achieved through degradation of this host resistance factor by a bacterial virulence factor. However, we did not observe any reduction in protein levels of the IRG proteins Irgb10, Irga6, Irgm1, or Irgm3 in *C. muridarum*-infected cells (J. Coers, unpublished data). Alternatively, *C. muridarum* may modify the biochemical properties of Irgb10 required for membrane binding. Interestingly, the N-terminal peptide of Irgb10, MGQSSSKPDAKAHNMASS-, constitutes a highly probable site for myristoylation and, based on the structure-function analysis of another myristoylated IRG protein, Irga6, this lipid modification is most likely required for membrane targeting (30). Although no eukaryotic or bacterial demyristoylation enzymes are known to exist, changes in protein conformation can sequester the myristate moiety in a hydrophobic pocket within the protein to cause membrane detachment, a mechanism referred to as the "myristoyl switch" (53). The best described example for myristoyl switching is the regulation of membrane binding of the GTPase ADP ribosylation factor-1 (Arf-1) through alternative binding of GDP and GTP (54, 55). A similar myristoyl switch can easily be envisioned for myristoylated IRG proteins that are known to bind both GDP and GTP (51). Future studies should explore the effect of *C. muridarum* infections on the ratio of GTP- and GDP-bound forms of Irgb10 and Irga6 in host cells. Lastly, it is also conceivable that a bacterial effector molecule derived from *C. muridarum* targets not Irgb10 directly but a separate host factor required for localization of Irgb10 to the *Chlamydia* inclusion.

An important unanswered question is the identity of the bacterial effector molecule(s) required for the evasion of the IRG-mediated antimicrobial host responses by *C. muridarum*. Because *C. muridarum* blocks Irgb10 localization to *C. trachomatis* inclusions only in coinfected cells, we suggest that *C. muridarum* secrets an

inhibitory factor directly into the host cell (and not into the medium). Although *C. muridarum* can inhibit Irgb10 accumulation at *C. trachomatis* inclusions in *trans* (between two inclusions in the same cell), an efficient reduction in the number of Irgb10$^+$ *C. trachomatis* inclusions requires the two *Chlamydia* species to reside in the same inclusion. To explain these results, we propose the existence of a factor secreted by *C. muridarum* into the cytosol and the subsequent association of this factor with the inclusion membrane. If two inclusions are in close proximity to one another, this putative factor may associate with a *C. trachomatis* inclusion in *trans* and inhibit Irgb10 localization to the *C. trachomatis* inclusion. The rare occurrence of Irgb10$^+$ fused inclusions (containing *C. muridarum* and *C. trachomatis*) could be a consequence of *C. muridarum* inclusions fusing with *C. trachomatis* inclusions that have already acquired Irgb10.

It has previously been proposed that a cytotoxin containing a domain with sequence homology to the *Yersinia*-derived virulence factor YopT may be the bacterial factor responsible for immune evasion (13). This hypothesis was based on the argument that *Yersinia*-derived YopT binds to and proteolytically inactivates prenylated Rho GTPases and that the GTPase Irga6 is the only IRG containing a C-terminal peptide sequence (-CLRN) that is reminiscent of a CaaX isoprenylation sequence (13). The authors therefore suggested that the *Chlamydia* YopT homologue TC438 could inactivate Irga6 through cleavage of the lipidic moiety and thus confer resistance to the murine IFN-γ response (13). However, this curious hypothesis was constructed in the absence of any experimental evidence for prenylation of Irga6 and failed to consider that the arginine in the penultimate position of the -CLRN sequence made prenylation of Irga6 unlikely (56). Furthermore, we have shown here that inactivation of Irga6 cannot be sufficient to achieve immune evasion. Moreover, despite carrying a YopT homologue in its genome, another *Chlamydia* strain, *Chlamydia caviae*, is sensitive to IFN-γ treatment in mouse cells (45). Collectively, these data refute the model proposed by Nelson et al (13). Although it cannot be excluded that the *Chlamydia* YopT homologue plays a role in immune evasion, we need to consider other *C. muridarum* genes as the mediators of immune escape from the murine IFN-γ response.

Members of the IRG family are key mediators of host resistance to a large number of intracellular bacterial and protozoan pathogens in mice (36, 38, 40). At least 23 IRG genes are found in the mouse genome (34). In contrast, humans possess only two IRG genes: IRGC, which is exclusively expressed in the male gonad similarly as its mouse ortholog, and IRGM, which is a truncated, noninducible ortholog of the mouse Irgm subclass (34). Surprisingly, human IRGM, despite its truncation and lack of IFN-mediated induction, has been implicated in cell-autonomous resistance to *Mycobacteria* and shown to play a role in the induction of autophagy (57). However, the relative subtlety of the observed phenotype of IRGM-depleted human cells compared with the astonishing phenotypes of the IRG knockout mice suggests that IRG-mediated immunity is of far less importance in humans than it is in mice. Because functional IRG genes appear to be the norm for mammalian genomes (34), the lack of an IFN-inducible, IRG-mediated immune response in primates is surprising and raises questions concerning the evolution of the IRG family. It is currently unclear whether other molecules or distinct pathways in humans substitute functionally for the IRG-dependent branch of the IFN-γ response. Remarkably, the IRG protein Irgm1 has recently been shown to play a role as a negative regulator of proinflammatory signaling in mice (58), and at the same time a separate study showed significant association of a single nucleotide polymorphism in human IRGM with the autoinflammatory syndrome Crohn's disease (59). Therefore, it is conceivable that the anti-inflammatory function of Irgm1 has been preserved in humans while the antimicrobial function of IRG proteins is largely absent. The apparent difference in the IFN-γ responses of mice and men is another example for the remarkable divergence in the immune responses of two relatively closely related host species (60). This variability in host immune responses creates a formidable obstacle for pathogens to cross from one host species to another and may be an important factor in shaping the host tropism of pathogens.

Acknowledgments

We thank Kerry McAuliffe for technical assistance and David Gondek and Bethany Mingle for critical reading of the manuscript.

Disclosures

The authors have no financial conflict of interest.

References

1. Belland, R., D. M. Ojcius, and G. I. Byrne. 2004. *Chlamydia*. *Nat. Rev. Microbiol.* 2: 530–531.
2. Resnikoff, S., D. Pascolini, D. Etya'ale, I. Kocur, R. Pararajasegaram, G. P. Pokharel, and S. P. Mariotti. 2004. Global data on visual impairment in the year 2002. *Bull. W. H. O.* 82: 844–851.
3. World Health Organization. 2001. Global prevalence and incidence of selected curable sexually transmitted infections: overview and estimates. *World Health Organization*, Geneva. p. 10.
4. Brunham, R. C., and J. Rey-Ladino. 2005. Immunology of *Chlamydia* infection: implications for a *Chlamydia trachomatis* vaccine. *Nat. Rev. Immunol.* 5: 149–161.
5. McClarty, G., H. D. Caldwell, and D. E. Nelson. 2007. Chlamydial interferon γ immune evasion influences infection tropism. *Curr. Opin. Microbiol.* 10: 47–51.
6. Morrison, R. P., and H. D. Caldwell. 2002. Immunity to murine chlamydial genital infection. *Infect. Immun.* 70: 2741–2751.
7. Abdelrahman, Y. M., and R. J. Belland. 2005. The chlamydial developmental cycle. *FEMS Microbiol. Rev.* 29: 949–959.
8. Fields, K. A., and T. Hackstadt. 2002. The chlamydial inclusion: escape from the endocytic pathway. *Annu. Rev. Cell. Dev. Biol.* 18: 221–245.
9. Read, T. D., R. C. Brunham, C. Shen, S. R. Gill, J. F. Heidelberg, O. White, E. K. Hickey, J. Peterson, T. Utterback, K. Berry, et al. 2000. Genome sequences of *Chlamydia trachomatis* MoPn and *Chlamydia pneumoniae* AR39. *Nucleic Acids Res.* 28: 1397–1406.
10. Read, T. D., G. S. Myers, R. C. Brunham, W. C. Nelson, I. T. Paulsen, J. Heidelberg, E. Holtzapple, H. Khouri, N. B. Federova, H. A. Carty, et al. 2003. Genome sequence of *Chlamydophila caviae* (*Chlamydia psittaci* GPIC): examining the role of niche-specific genes in the evolution of the Chlamydiaceae. *Nucleic Acids Res.* 31: 2134–2147.
11. Stephens, R. S., S. Kalman, C. Lammel, J. Fan, R. Marathe, L. Aravind, W. Mitchell, L. Olinger, R. L. Tatusov, Q. Zhao, et al. 1998. Genome sequence of an obligate intracellular pathogen of humans: *Chlamydia trachomatis*. *Science* 282: 754–759.
12. Morrison, R. P. 2000. Differential sensitivities of *Chlamydia trachomatis* strains to inhibitory effects of γ interferon. *Infect. Immun.* 68: 6038–6040.
13. Nelson, D. E., D. P. Virok, H. Wood, C. Roshick, R. M. Johnson, W. M. Whitmire, D. D. Crane, O. Steele-Mortimer, L. Kari, G. McClarty, and H. D. Caldwell. 2005. Chlamydial IFN-γ immune evasion is linked to host infection tropism. *Proc. Natl. Acad. Sci. USA* 102: 10658–10663.
14. Roshick, C., H. Wood, H. D. Caldwell, and G. McClarty. 2006. Comparison of γ interferon-mediated antichlamydial defense mechanisms in human and mouse cells. *Infect. Immun.* 74: 225–238.
15. Fehlner-Gardiner, C., C. Roshick, J. H. Carlson, S. Hughes, R. J. Belland, H. D. Caldwell, and G. McClarty. 2002. Molecular basis defining human *Chlamydia trachomatis* tissue tropism: a possible role for tryptophan synthase. *J. Biol. Chem.* 277: 26893–26903.
16. Taylor, M. W., and G. S. Feng. 1991. Relationship between interferon-γ, indoleamine 2,3-dioxygenase, and tryptophan catabolism. *FASEB J.* 5: 2516–2522.
17. Thomas, S. M., L. F. Garrity, C. R. Brandt, C. S. Schobert, G. S. Feng, M. W. Taylor, J. M. Carlin, and G. I. Byrne. 1993. IFN-γ-mediated antimicrobial response: indoleamine 2,3-dioxygenase-deficient mutant host cells no longer inhibit intracellular *Chlamydia* spp. or *Toxoplasma* growth. *J. Immunol.* 150: 5529–5534.
18. Beatty, W. L., T. A. Belanger, A. A. Desai, R. P. Morrison, and G. I. Byrne. 1994. Tryptophan depletion as a mechanism of γ interferon-mediated chlamydial persistence. *Infect. Immun.* 62: 3705–3711.
19. Beatty, W. L., R. P. Morrison, and G. I. Byrne. 1994. Persistent chlamydiae: from cell culture to a paradigm for chlamydial pathogenesis. *Microbiol. Rev.* 58: 686–699.
20. Caldwell, H. D., H. Wood, D. Crane, R. Bailey, R. B. Jones, D. Mabey, I. Maclean, Z. Mohammed, R. Peeling, C. Roshick, et al. 2003. Polymorphisms in *Chlamydia trachomatis* tryptophan synthase genes differentiate between genital and ocular isolates. *J. Clin. Invest.* 111: 1757–1769.
21. Bernstein-Hanley, I., J. Coers, Z. R. Balsara, G. A. Taylor, M. N. Starnbach, and W. F. Dietrich. 2006. The p47 GTPases Igtp and Irgb10 map to the *Chlamydia*

trachomatis susceptibility locus Ctrq-3 and mediate cellular resistance in mice. *Proc. Natl. Acad. Sci. USA* 103: 14092–14097.
22. Shao, F., P. O. Vacratsis, Z. Bao, K. E. Bowers, C. A. Fierke, and J. E. Dixon. 2003. Biochemical characterization of the *Yersinia* YopT protease: cleavage site and recognition elements in Rho GTPases. *Proc. Natl. Acad. Sci. USA* 100: 904–909.
23. Collazo, C. M., G. S. Yap, G. D. Sempowski, K. C. Lusby, L. Tessarollo, G. F. Woude, A. Sher, and G. A. Taylor. 2001. Inactivation of LRG-47 and IRG-47 reveals a family of interferon γ-inducible genes with essential, pathogen-specific roles in resistance to infection. *J. Exp. Med.* 194: 181–188.
24. Taylor, G. A., C. M. Collazo, G. S. Yap, K. Nguyen, T. A. Gregorio, L. S. Taylor, B. Eagleson, L. Secrest, E. A. Southon, S. W. Reid, et al. 2000. Pathogen-specific loss of host resistance in mice lacking the IFN-γ-inducible gene IGTP. *Proc. Natl. Acad. Sci. USA* 97: 751–755.
25. Martens, S., I. Parvanova, J. Zerrahn, G. Griffiths, G. Schell, G. Reichmann, and J. C. Howard. 2005. Disruption of *Toxoplasma gondii* parasitophorous vacuoles by the mouse p47-resistance GTPases. *PLoS Pathog.* 1: e24.
26. Parvanova, I. 2005. Analysis of the role of the p47 GTPase IIGP1 in resistance against intracellular pathogens. Doctoral dissertation, University of Cologne, Cologne, Germany.
27. Bernstein-Hanley, I., Z. R. Balsara, W. Ulmer, J. Coers, M. N. Starnbach, and W. F. Dietrich. 2006. Genetic analysis of susceptibility to *Chlamydia trachomatis* in mouse. *Genes Immun.* 7: 122–129.
28. Howard, L., N. S. Orenstein, and N. W. King. 1974. Purification on renografin density gradients of *Chlamydia trachomatis* grown in the yolk sac of eggs. *Appl. Microbiol.* 27: 102–106.
29. Cotter, T. W., Q. Meng, Z. L. Shen, Y. X. Zhang, H. Su, and H. D. Caldwell. 1995. Protective efficacy of major outer membrane protein-specific immunoglobulin A (IgA) and IgG monoclonal antibodies in a murine model of *Chlamydia trachomatis* genital tract infection. *Infect. Immun.* 63: 4704–4714.
30. Martens, S., K. Sabel, R. Lange, R. Uthaiah, E. Wolf, and J. C. Howard. 2004. Mechanisms regulating the positioning of mouse p47 resistance GTPases LRG-47 and IIGP1 on cellular membranes: retargeting to plasma membrane induced by phagocytosis. *J. Immunol.* 173: 2594–2606.
31. Butcher, B. A., R. I. Greene, S. C. Henry, K. L. Annecharico, J. B. Weinberg, E. Y. Denkers, A. Sher, and G. A. Taylor. 2005. p47 GTPases regulate *Toxoplasma gondii* survival in activated macrophages. *Infect. Immun.* 73: 3278–3286.
32. Taylor, G. A., M. Jeffers, D. A. Largaespada, N. A. Jenkins, N. G. Copeland, and G. F. Woude. 1996. Identification of a novel GTPase, the inducibly expressed GTPase, that accumulates in response to interferon γ. *J. Biol. Chem.* 271: 20399–20405.
33. Miyairi, I., V. R. Tatireddigari, O. S. Mahdi, L. A. Rose, R. J. Belland, L. Lu, R. W. Williams, and G. I. Byrne. 2007. The p47 GTPases Iigp2 and Irgb10 regulate innate immunity and inflammation to murine *Chlamydia psittaci* infection. *J. Immunol.* 179: 1814–1824.
34. Bekpen, C., J. P. Hunn, C. Rohde, I. Parvanova, L. Guethlein, D. M. Dunn, E. Glowalla, M. Leptin, and J. C. Howard. 2005. The interferon-inducible p47 (IRG) GTPases in vertebrates: loss of the cell autonomous resistance mechanism in the human lineage. *Genome Biol.* 6: R92.
35. Feng, C. G., C. M. Collazo-Custodio, M. Eckhaus, S. Hieny, Y. Belkaid, K. Elkins, D. Jankovic, G. A. Taylor, and A. Sher. 2004. Mice deficient in LRG-47 display increased susceptibility to mycobacterial infection associated with the induction of lymphopenia. *J. Immunol.* 172: 1163–1168.
36. MacMicking, J. D. 2004. IFN-inducible GTPases and immunity to intracellular pathogens. *Trends Immunol.* 25: 601–609.
37. MacMicking, J. D., G. A. Taylor, and J. D. McKinney. 2003. Immune control of tuberculosis by IFN-γ-inducible LRG-47. *Science* 302: 654–659.
38. Martens, S., and J. Howard. 2006. The interferon-inducible GTPases. *Annu. Rev. Cell. Dev. Biol.* 22: 559–589.
39. Santiago, H. C., C. G. Feng, A. Bafica, E. Roffe, R. M. Arantes, A. Cheever, G. Taylor, L. Q. Vieira, J. Aliberti, R. T. Gazzinelli, and A. Sher. 2005. Mice deficient in LRG-47 display enhanced susceptibility to *Trypanosoma cruzi* infection associated with defective hemopoiesis and intracellular control of parasite growth. *J. Immunol.* 175: 8165–8172.
40. Taylor, G. A., C. G. Feng, and A. Sher. 2004. p47 GTPases: regulators of immunity to intracellular pathogens. *Nat. Rev. Immunol.* 4: 100–109.
41. Ling, Y. M., M. H. Shaw, C. Ayala, I. Coppens, G. A. Taylor, D. J. Ferguson, and G. S. Yap. 2006. Vacuolar and plasma membrane stripping and autophagic elimination of *Toxoplasma gondii* in primed effector macrophages. *J. Exp. Med.* 203: 2063–2071.
42. Taylor, G. A., R. Stauber, S. Rulong, E. Hudson, V. Pei, G. N. Pavlakis, J. H. Resau, and G. F. Vande Woude. 1997. The inducibly expressed GTPase localizes to the endoplasmic reticulum, independently of GTP binding. *J. Biol. Chem.* 272: 10639–10645.
43. Zerrahn, J., U. E. Schaible, V. Brinkmann, U. Guhlich, and S. H. Kaufmann. 2002. The IFN-inducible Golgi- and endoplasmic reticulum- associated 47-kDa GTPase IIGP is transiently expressed during listeriosis. *J. Immunol.* 168: 3428–3436.
44. Gutierrez, M. G., S. S. Master, S. B. Singh, G. A. Taylor, M. I. Colombo, and V. Deretic. 2004. Autophagy is a defense mechanism inhibiting BCG and *Mycobacterium tuberculosis* survival in infected macrophages. *Cell* 119: 753–766.
45. Nelson, D. E., L. D. Taylor, J. G. Shannon, W. M. Whitmire, D. D. Crane, G. McClarty, H. Su, L. Kari, and H. D. Caldwell. 2007. Phenotypic rescue of *Chlamydia trachomatis* growth in IFN-γ treated mouse cells by irradiated *Chlamydia muridarum*. *Cell. Microbiol.* 9: 2289–2298.
46. Finlay, B. B., and G. McFadden. 2006. Anti-immunology: evasion of the host immune system by bacterial and viral pathogens. *Cell* 124: 767–782.
47. Sansonetti, P. J., and J. P. Di Santo. 2007. Debugging how bacteria manipulate the immune response. *Immunity* 26: 149–161.
48. Chakravortty, D., I. Hansen-Wester, and M. Hensel. 2002. *Salmonella* pathogenicity island 2 mediates protection of intracellular *Salmonella* from reactive nitrogen intermediates. *J. Exp. Med.* 195: 1155–1166.
49. Haley, B., and P. D. Zamore. 2004. Kinetic analysis of the RNAi enzyme complex. *Nat. Struct. Mol. Biol.* 11: 599–606.
50. Jackson, A. L., S. R. Bartz, J. Schelter, S. V. Kobayashi, J. Burchard, M. Mao, B. Li, G. Cavet, and P. S. Linsley. 2003. Expression profiling reveals off-target gene regulation by RNAi. *Nat. Biotechnol.* 21: 635–637.
51. Uthaiah, R. C., G. J. Praefcke, J. C. Howard, and C. Herrmann. 2003. IIGP1, an interferon-γ-inducible 47-kDa GTPase of the mouse, showing cooperative enzymatic activity and GTP-dependent multimerization. *J. Biol. Chem.* 278: 29336–29343.
52. Rzomp, K. A., L. D. Scholtes, B. J. Briggs, G. R. Whittaker, and M. A. Scidmore. 2003. Rab GTPases are recruited to chlamydial inclusions in both a species-dependent and species-independent manner. *Infect. Immun.* 71: 5855–5870.
53. Resh, M. D. 1999. Fatty acylation of proteins: new insights into membrane targeting of myristoylated and palmitoylated proteins. *Biochim. Biophys. Acta* 1451: 1–16.
54. Amor, J. C., D. H. Harrison, R. A. Kahn, and D. Ringe. 1994. Structure of the human ADP-ribosylation factor 1 complexed with GDP. *Nature* 372: 704–708.
55. Goldberg, J. 1999. Structural and functional analysis of the ARF1-ARFGAP complex reveals a role for coatomer in GTP hydrolysis. *Cell* 96: 893–902.
56. Reiss, Y., S. J. Stradley, L. M. Gierasch, M. S. Brown, and J. L. Goldstein. 1991. Sequence requirement for peptide recognition by rat brain $p21^{ras}$ protein farnesyltransferase. *Proc. Natl. Acad. Sci. USA* 88: 732–736.
57. Singh, S. B., A. S. Davis, G. A. Taylor, and V. Deretic. 2006. Human IRGM induces autophagy to eliminate intracellular mycobacteria. *Science* 313: 1438–1441.
58. Bafica, A., C. G. Feng, H. C. Santiago, J. Aliberti, A. Cheever, K. E. Thomas, G. A. Taylor, S. N. Vogel, and A. Sher. 2007. The IFN-inducible GTPase LRG47 (Irgm1) negatively regulates TLR4-triggered proinflammatory cytokine production and prevents endotoxemia. *J. Immunol.* 179: 5514–5522.
59. Parkes, M., J. C. Barrett, N. J. Prescott, M. Tremelling, C. A. Anderson, S. A. Fisher, R. G. Roberts, E. R. Nimmo, F. R. Cummings, D. Soars, et al. 2007. Sequence variants in the autophagy gene IRGM and multiple other replicating loci contribute to Crohn's disease susceptibility. *Nat. Genet.* 39: 830–832.
60. Mestas, J., and C. C. Hughes. 2004. Of mice and not men: differences between mouse and human immunology. *J. Immunol.* 172: 2731–2738.